https://doi.org/10.14669/AM/218873

REDUNDANT CONSTRAINTS IN THE DISC-TYPE AUTOMOTIVE BRAKE MECHANISMS: INFLUENCE AND ELIMINATION

VLADYSLAV PROTSENKO[1], SERGIY RUSANOV[2], GLIB SHIKAREV[3]

Abstract

The article deals with the analysis of possible causes of vehicle yaw during braking as one of the phenomena affecting passenger safety. The braking diagram of the vehicle and the change in vehicle deceleration during the braking process are analyzed. Based on the analysis of the wheel brake mechanism's structure, the identification of the number and location of redundant constraints, their possible influence on the mechanism's operation and braking process, is demonstrated. Notably, the existing redundant constraints can cause an abnormal load, leading to the operation of parts with unintended preloads and tensions, and thereby reducing the service life of brake parts and compromising the safety of the vehicle braking process. Using constructive methods by changing the structure of the mechanism, adding kinematic pair motions and using kinematic connections, three variants of new brake mechanism designs are proposed, which reduce the number of redundant links and can have a significant positive influence on brake operation.

Keywords: brake mechanism; vehicle yaw; braking intensity; deceleration; redundant constraint; load unevenness

1. Introduction

Vehicle braking is one of the most hazardous driving modes, as it may result in the vehicle leaving the corridor, whose width is set at 3.5 m by [1]. It is evident that when vehicles

[1] Transport Systems and Technical Service, Kherson National Technical University Kherson, Ukraine, email: 1904pvo@gmail.com, ORCID: 0000-0002-3468-4952

[2] Transport Systems and Technical Service, Kherson National Technical University Kherson, Ukraine, email: ohvpbm@i.ua, ORCID: 0000-0002-1003-4867

[3] Transport Systems and Technical Service, Kherson National Technical University Kherson, Ukraine, email: glibshikarev@gmail.com, ORCID: 0009-0006-2797-5459

https://doi.org/10.14669/AM/218873

traveling toward each other are braking simultaneously, the danger only increases. The significance of the investigated process is emphasized by the sustained attention it has received in scientific publications. In the article [2] a new strategy of vehicle yaw moment control is proposed, which is based on the brake-by-wire system in order to increase the stability of the vehicle in complex maneuvers and driving conditions. The strategy is aimed at ensuring control of the yaw rate and sideslip angle at times when the wheels and tire may lose traction, for example, during sharp braking or changes in the trajectory of movement. A method of calculating the additional yaw moment based on the deviations of the actual yaw angle and sideslip from the target values is proposed. The difference between the desired and actual values of these parameters is used as an input for the controller. The controller uses a fuzzy logic controller to generate a corrective yaw moment, which is transmitted to the corresponding wheels to stabilize the vehicle movement. The article also presents a series of simulation and experimental verifications of the proposed strategy. The tests included various road situations: sharp steering input, double lane change maneuver, turns, etc. The results showed that after applying brake-by-wire yaw control, there was an improvement in vehicle stability and handling. The authors note that the proposed approach has the potential for integration into modern active vehicle safety systems. In study [3], the influence of braking force distribution among the wheels on vehicle yaw behavior and overall stability under combined braking and steering conditions is investigated. Particular attention is paid to the interaction between asymmetric braking forces and the vehicle's lateral dynamics, which can lead to increased yaw rate and sideslip angle, especially at high speeds and under limited road adhesion. The results show that integrated control reduces yaw rate and sideslip angle oscillations by 15–25% compared to conventional braking control. The redistribution of braking forces enables a more uniform utilization of tire–road friction, preventing premature wheel lock-up and the development of unstable yaw motion. As a result, the vehicle maintains directional stability during braking in a turn, and trajectory deviation is significantly reduced compared to operation without active brake force redistribution. The study confirms that wheel-level braking force control is an effective tool for yaw suppression during complex combined maneuvers. Study [4] investigates the impact of brake force redistribution on vehicle directional stability during braking in the event of a failure of one braking mechanism. The authors consider a vehicle equipped with a brake-by-wire system and analyze how braking force asymmetry leads to an increase in yaw moment and sideslip angle during intensive braking. It is shown that, in the absence of brake force redistribution, the failure of one brake results in a more than 25–30% increase in the maximum yaw rate compared to nominal braking conditions. The application of the proposed control algorithm reduces the peak yaw rate by 15–20% and decreases the sideslip angle by more than 10%. At the same time, braking efficiency is maintained at 85–90% of the normal fault-free level. The response time of the brake force redistribution system is approximately 0.1–0.2 s, ensuring vehicle stabilization at an early stage of instability development. The obtained results confirm that targeted redistribution of braking forces among the wheels is an effective means of yaw suppression during emergency braking conditions. In study [5], the effect of coordinated braking force distribution among the wheels on the directional stability of an

https://doi.org/10.14669/AM/218873

electric vehicle during braking, including partial brake actuator failure scenarios, is examined. The authors address the problem of significant yaw moments and lateral vehicle deviation caused by asymmetric braking and aim to minimize these effects through the integration of electronic brake force distribution and direct yaw moment control. The results show that coordinated brake force distribution reduces the braking distance by 7.05% compared to the uncontrolled mode. In addition, the maximum lateral deviation associated with yaw development is reduced by 26.74%. The average longitudinal deceleration remains within the range of 3.5–4.1 m/s² even in the presence of a single brake channel failure, indicating high braking effectiveness. Peak yaw rate values are reduced to a stable range, preventing the vehicle from transitioning into an uncontrollable skid. Thus, the study demonstrates that coordinated redistribution of braking forces among the wheels significantly mitigates the impact of braking asymmetry on vehicle yaw and enhances directional stability under emergency conditions. In study [6], the influence of coordinated braking force control on the directional stability of an in-wheel-motor electric vehicle during braking is investigated. The authors analyze how uncoordinated braking force distribution between the front and rear axles leads to undesirable yaw moments and increased sideslip angles, particularly under low-adhesion conditions. The results indicate that optimized braking force distribution reduces the generated yaw moment by 15–18% compared to a fixed distribution scheme. The maximum yaw angle is reduced to 0.10–0.12 rad, whereas in the absence of coordination it reaches 0.15–0.18 rad. This results in more stable vehicle deceleration and a reduced risk of skid development. The study demonstrates that braking force coordination among the wheels in in-wheel-motor electric vehicles is a key factor in improving directional stability during braking. The systems mentioned in the previous studies do not address the root causes of braking force oscillations; instead, they only partially mitigate their consequences, while their implementation requires additional resources.

Below is the analysis of braking diagrams (Figure 1) obtained for an M1 category vehicle, conducted under proving-ground conditions on a certified road section with a flat, horizontal asphalt-concrete pavement. A measurement system was used to record acceleration, speed, as well as to register the vehicle trajectory and braking distance. The system included, in particular, a professional GPS receiver connected to a computer equipped with the required software, an antenna for receiving signals from the GPS satellite system, and other auxiliary components. It makes it possible to establish that at the beginning of the braking process ($t = 0$, $V_0 = 42.55$ km/h) the lateral acceleration a_l has a nonzero negative value (–0.207 m/s²), which means that the initial lateral velocity of the vehicle is also nonzero and begins to change direction with the onset of braking. The lateral acceleration a_l varies in magnitude and sign periodically, with the period increasing from 0.2 s at the beginning of the braking process to 0.5 s at its end, while the amplitude initially increases and then decreases. Changes in the longitudinal a_f and lateral a_l accelerations occur in the same phase, indicating that the lateral acceleration depends on the intensity of the wheel brake mechanisms' operation.

https://doi.org/10.14669/AM/218873

Regarding the analysis of the reasons for this behavior of the braking process, our hypothesis is that the reason for the periodic change in transverse acceleration a_l and, consequently, vehicle yaw during braking may be the periodic increase in the friction torque of the wheel brake mechanisms, for example due to axial runout of the brake discs and/or misalignment or sticking of the brake calipers, or uneven wear of the brake pads. This hypothesis is supported by the following:

- the presence of negative lateral acceleration at the beginning of the braking process (the vehicle was already drifting to the left before braking due to higher resistance of the front left and rear right wheels). This should not occur in the absence of resistance to the rotation of these wheels;
- the period of variation of the lateral acceleration is of the same order as the wheel rotation period (with the period increasing as the wheels reduce their rotational speed during braking).

In existing brake mechanism designs, the presence of disc axial runout, misalignments, uneven pad wear, and manufacturing tolerances is not practically compensated for, since the design of brake mechanisms allows these imperfections and wear effects to influence the braking process, in some cases generating a braking torque even in the absence of pads clamping against the disc. All this is explained by the lack of self-alignment capability of the components.

A significant number of scientific studies published in recent years have focused on investigating methods and means to enhance the wear resistance of brake mechanism elements through materials science and design approaches.

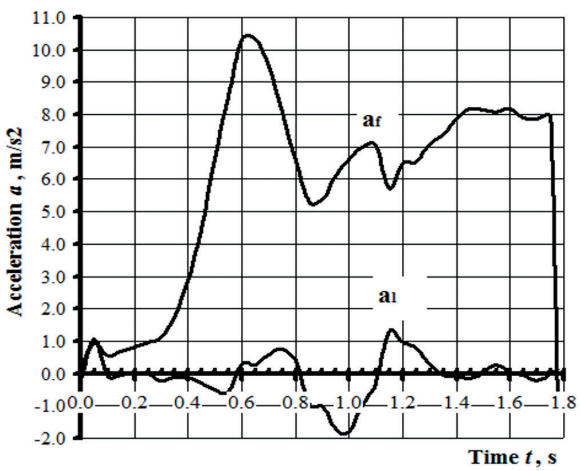

Fig. 1. Experimental graphs of changes in vehicle deceleration during braking (a_f – longitudinal acceleration, a_l – lateral acceleration)

https://doi.org/10.14669/AM/218873

In the article [7] the prediction of wear of brake pads of the car and estimation of their residual resource (RUL) based on the operation data, as well as the influence of changes in the mass of the vehicle on the wear process is considered. The authors built a model that uses data on real mileage (about 10200 km) and measurements of pad thickness on 31 samples, and also combines signals from on-board diagnostics, inertial measurement unit (IMU) and GPS data to estimate the braking force and wear. The main approach is to use a model of longitudinal dynamics of the vehicle to estimate the overall braking performance. Such an estimate allows to simulate the rate of pad wear, since wear is directly related to the total energy absorbed by the brakes. At the same time, the authors integrate for the first time a real estimate of the mass of the car into the model (mass change up to 23% of the nominal), which improves the accuracy of wear prediction under variable load conditions. Detailed experimental data were used to build the model, and the simulation results were verified on a separate part of the collected measurements. The developed model showed that estimating the vehicle mass allows reducing the errors in predicting the remaining life of the pads, as well as more accurately characterizing their wear under different driving modes. This opens up opportunities for optimizing maintenance and improving road transport safety, especially when using sensors and real-time monitoring systems.

Other studies were carried out in [8], the performance efficiency of a disc brake mechanism of a *Hyundai Accent* vehicle was investigated by modeling various driving and braking modes on test benches. The modeling was performed using front disc brake pads from different manufacturers. The obtained results show that, depending on the manufacturer, the wear characteristics of brake pads and discs, as well as the magnitude of the braking torque, differ significantly.

Study [9] focuses on investigating the potential of using functionally graded ductile iron (FGDI) as a material for brake pads to enhance their wear resistance. The methodology consisted of two stages: controlled tribological tests conducted under laboratory conditions to identify wear mechanisms and evaluate friction coefficients, and bench tests on disc friction machines that simulated real braking conditions at various temperatures. Microscopic surface analysis revealed the formation of graphite plateaus on the pads and transfer films on the discs. It was established that FGDI with a functional gradient demonstrated higher wear resistance, a more stable friction coefficient, and lower sensitivity to temperature variations.

In a study [10], the relationship between brake pad and disc wear, as well as the efficiency of the vehicle braking system, was analyzed. The methodology included field tests on a vehicle (intensive and moderate operation modes) and bench tests on a dynamometric stand. During the study, the thickness of the pad friction material was measured (for example, front pads wore from 13 mm to nearly 10 mm after 18.5 thousand km of mileage), braking force was recorded, and braking system efficiency was evaluated as a percentage (the ratio of braking force to vehicle mass). It was found that after 18.5 thousand km of urban driving, braking system efficiency was about 59%, while after replacing the discs and pads, it increased to

https://doi.org/10.14669/AM/218873

72%. Thus, it was demonstrated that pad/disc wear has a significant effect on braking system performance.

In [11], the tribological properties and wear of disc–pad friction pairs were investigated on a laboratory test rig. Several types of pad and disc materials (types A, B, C, D, E, F) were analyzed in the temperature range of 100–450°C with a step of 50°C. The aim was to determine how the composition of the friction material affects disc wear and changes in the friction coefficient under thermal loading. It was found that the ratio of maximum to minimum disc wear varied from 6.0 to 10.0, depending on the material. At 800 and 1000 braking cycles and temperatures of 100–250°C/100–450°C, the corresponding ratios were 7.6 and 14.0. Thus, it was demonstrated that conventional pad materials (types A–D) result in higher disc wear in the second temperature regime, whereas materials E and F exhibit greater stability. It is recommended to select pad compositions taking into account their effect on the disc and the thermal regime.

In [12], a method for influencing the wear resistance of brake discs using ultrasonic vibrations during casting of disc blanks (frequencies of 20 kHz and 25 kHz) is proposed to improve friction and wear properties. Bench studies employed pressure, speed, and temperature sensors to measure the average friction coefficient and its stability under various braking conditions. The results show that discs manufactured using ultrasonic treatment exhibited better property stability and reduced wear rate compared to standard discs. It should be noted that the use of additional processing during blank manufacturing increases disc cost and, consequently, vehicle operating costs.

In the article [13] a new method for diagnosing and localizing changes in the thickness and corrosion of a car brake disc based on data collected during normal vehicle operation is proposed. Defects such as uneven disc thickness and corrosion damage are among the most common causes of brake judder – unwanted vibrations of the pedal, steering wheel and body during braking, which significantly affects the comfort and safety of driving, as it can lead to yaw during braking. The aim of the study was to develop an online method for assessing the condition of the disc to reduce the costs of scheduled technical inspections in fleets or when servicing autonomous vehicles. The authors performed the conversion of signals from vehicle sensors (brake pressure, brake force extension, acceleration extension and wheel speed) from the time domain to the angle domain. This allowed to identify parameters sensitive to disc degradation, such as signal dispersion, envelope and spectral indices in the angle domain. The system also demonstrates high robustness to external noise caused by changes in tire type, tire pressure and vehicle mass, ensuring diagnostic stability under various operating conditions. The methodology also includes a classification model that integrates various condition indicators and is able to identify the least healthy disc with separate detection for each wheel (corner isolation). This allows not only to detect the problem, but also to localize the weak point of the braking system, which is useful for scheduled maintenance or for adaptive safety control.

https://doi.org/10.14669/AM/218873

Article [14] analyzes friction and wear processes in the disc–pad pair under high-load conditions. It was established that maximum local pad wear depth occurs in critical areas (edges of friction surfaces); wear intensity increases rapidly in the initial phase and then decreases. Radial wear decreases from the outer to the inner edge due to the linear increase in circumferential speed with radius. As a result, asymmetric contact pressure distribution across the disc and local thermal effects lead to the formation of "hot rings" along the radius and the occurrence of DTV.

Study [15] assesses the influence of DTV and OOR (out-of-roundness) on the operation of electromechanical brakes (EMB). Analytical models and a brake simulation model incorporating EMB motor–gear stiffness were used, along with bench experiments with artificially introduced errors. It was demonstrated that the critical harmfulness threshold of DTV for EMB systems is lower than that of conventional hydraulic calipers; specifically, at DTV>36 μm, noticeable additional dynamic loads on motor–gear units and increased bearing loads are observed. OOR on the order of hundredths of a millimeter forms non-uniform radial contact, promoting localized wear and the formation of periodic radial rings or segments with increased wear. Therefore, stricter control of DTV/OOR tolerances is required for EMB systems, making service life improvement especially important.

Paper [16] examines the phenomenon of "double" or wedge-shaped wear of brake pads in braking systems of freight railway wagons. It was found that devices intended to ensure uniform pad wear are often damaged; as a result, wagon brake pads experience wedge-shaped wear: the upper edges are more heavily loaded and come into contact with the wheel even in the released brake state. This creates additional friction, accelerates wear, and disrupts its uniformity.

Study [17] focuses on the statistical analysis of geometric wear parameters of brake pads in modernized freight wagon braking systems. By collecting data from maintenance station checkpoints, wear-versus-mileage relationships were constructed using statistical methods. The results showed that after modernization of braking systems with improved wear-uniformity measures, pad service life increased by approximately 2.6 times. Thus, it was proven that improving wear uniformity through design methods leads to a significant increase in service life.

Thus, the service life of brake pads and discs can be increased not only by materials science methods, but also by improving the uniformity of wear of these elements, which depends, among other factors, on the uniformity of pressure in the contact zone. Pressure uniformity can be ensured by the self-alignment capability of brake mechanism components, or by the absence of redundant constraints in the mechanism. In study [18], the presence and influence of redundant constraints on the operation of brake mechanisms of lifting machines were analyzed. Disc and drum-type mechanisms were considered, and it was shown that most existing redundant constraints are angular; they require high manufacturing and

https://doi.org/10.14669/AM/218873

assembly accuracy of brake components, as well as strict parameter control during operation. Compensation for redundant constraints is usually achieved by increasing clearances in kinematic pairs, which leads to delayed brake actuation and the occurrence of dynamic loads during operation. Some redundant constraints prevent the self-alignment of brake pads relative to discs or drums. In the presence of disc runout, this may cause fluctuations in braking torque during braking and resistance to disc or drum rotation when the brake is released. For automotive brake mechanisms, studies on the mechanism structure could not be found, which creates conditions for further scientific research.

This work aims to analyze and improve the structural perfection of an automotive wheel disc brake mechanism by ensuring the self-alignment of its components.

The objectives of the study are:
- to develop a structural diagram of an automotive disc brake mechanism;
- to perform a structural analysis and determine the number and locations of redundant constraints;
- to assess the possible impact of the existing redundant constraints on the operation of the mechanism;
- to demonstrate the prospects for improving the brake mechanism by eliminating redundant constraints;
- to propose variants of modified brake mechanism designs with a reduced number of redundant constraints.

2. Methodology

Next, the disc brake mechanism of the *Daewoo Lanos* vehicle will be analyzed as a typical representative of such devices (Figure 2). It includes a brake disc 1, mounted with the ability to rotate relative to the vehicle suspension; an outer 2 and an inner 3 (with respect to the vehicle longitudinal axis) brake pad, installed on both sides of the brake disc 1 and capable of axial movement along the disc by means of their prismatic guide lugs sliding in the caliper slots, as well as interacting with the working surfaces of the disc faces through their friction surfaces; a brake caliper body 0, rigidly fixed relative to the suspension, into whose prismatic slots the prismatic guide lugs of the brake pads are inserted; a U-shaped brake caliper bracket 4, mounted on the caliper guides with the ability of axial movement, which on the outer side of the brake disc 1 can interact with the non-working side surface of the outer brake pad 2, and on the inner side of the brake disc 1, a piston 5 is installed in the axial bore of the caliper bracket 4 with the ability of axial movement, the piston being capable of interacting with its end face with the non-working side surface of the inner brake pad 3.

The described mechanism contains five movable links, $n = 5$ (disk 1, pads 2 and 3, bracket 4, and piston 5). Number of 5-class kinematic pairs here $P_5 = 1$ (O_5), number of 4-class kinematic

https://doi.org/10.14669/AM/218873

pairs $P_4 = 3$ [M_4, N_4, R_4], number of 3-class kinematic pairs $P3 = 8$ [A_3, B_3, C_3, D_3, E_3, F_3, L_3, K_3], 2 and 1-class kinematic pairs are absent – $P_2 = P_1 = 0$.

Total kinematic pairs number is:

$$P = P_5 + P_4 + P_3 + P_2 + P_1 = 1 + 3 + 8 + 0 + 0 = 12. \quad (1)$$

The sum of kinematic pairs movabilities:

$$f = 1P_5 + 2P_4 + 3P_3 + 4P_2 + 5P_1 = 1\times1 + 2\times3 + 3\times8 + 4\times0 + 5\times0 = 31. \quad (2)$$

Number of independent locked circuits by Gohman formula [19]:

$$k = P - n = 12 - 5 = 7. \quad (3)$$

Mechanism independent locked circuits are: $R_4F_3E_3D_3C_3R_4$; $M_4C_3D_3O_5M_4$; $N_4C_3D_3O_5N_4$; $A_3D_3B_3A_3$; $A_3C_3B_3A_3$; $K_3F_3L_3K_3$; $K_3E_3L_3K_3$.

Total mechanism mobility $W = W_b + W_l = 1 + 3 = 4$,
where $W_b = 1$ – basic mechanism mobility (disk 1 rotation around its axis);
$W_l = 3$ – local links mobilities (pads 2 and 3 movement, and piston 5 rotation).

a)

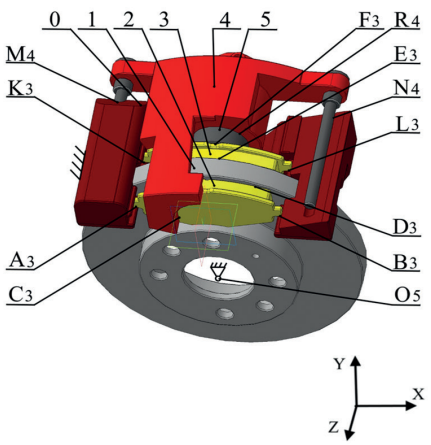

b)

Fig. 2. General view (a) and structural diagram (b) of wheel brake mechanism basic construction: 0 – brake caliper body; 1 – brake disc; 2 and 3 – outer and inner brake pads; 4 – shaped brake caliper bracket; 5 – piston

https://doi.org/10.14669/AM/218873

Then redundant constraints number in mechanism basic variant by Somov and Malyshev formula:

$$q_{SM} = W + 5P_5 + 4P_4 + 3P_3 + 2P_2 + P_1 - 6n = \\ = 4 + 5\times1 + 4\times3 + 3\times8 + 2\times0 + 0 - 6\times5 = 15. \tag{4}$$

Redundant constraints number by Ozols formula:

$$q_{OZ} = W + 6k - f = 4 + 6\times7 - 31 = 15. \tag{5}$$

The presented calculations are confirmed by the application of the L. Reshetov's circuit method [20] (Table 1). The main plane there is considered XY plane, the movabilities in this plane are indicated as planar [$f_p = f_x', f_y', f_z''$], and all others – as non-planar [$f_n = f_x'', f_y'', f_z'$]. The data in Table 1 indicate that most redundant constraints restrict the angular movabilities of the brake pads and therefore hinder their self-alignment relative to the discs (Table 2). This, together with uneven wear of the components, may lead to an increased non-uniformity of load distribution between them, which in turn can cause fluctuations in the friction torque of the wheel brake mechanisms and vehicle yaw during braking (what we saw in the Figure 1 diagrams). Redundant constraints may also result in off-design loading of mechanism elements, in particular assembly and operation with unintended preloads, which does not improve the performance of the brake mechanisms. In practice, the presence of redundant constraints is often compensated for by increasing clearances in kinematic pairs, which leads to delayed brake actuation and the occurrence of additional dynamic loads.

Tab. 1. Circuit method application to the wheel brake mechanism basic construction

Circuit	Planar movabilities f_p	Non-planar movabilities f_n
	f_x' f_y' f_z''	f_x'' f_y'' f_z'
$R_4F_3E_3D_3C_3R_4$	F F FR $W_t(5)$	Ø Ø R q_1 q_2
$M_4C_3D_3O_5M_4$	D D M	Ø Ø M q_3 q_4
$N_4C_3D_3O_5N_4$	Ø C NO $W_b(1)$ D	Ø Ø N q_5 q_6
$A_3D_3B_3A_3$	$W_t(2)$ AB Ø Ø q_7 q_8	Ø A A q_9
$A_3C_3B_3A_3$	C Ø C q_{10}	Ø B B q_{11}
$K_3F_3L_3K_3$	$W_t(3)$ KL Ø Ø q_{12} q_{13}	Ø K K q_{14}
$K_3E_3L_3K_3$	E E E	Ø L L q_{15}
	$W = 4,\ q = 15$	

https://doi.org/10.14669/AM/218873

Tab. 2. Redundant constraints influence the basic wheel brake mechanism construction

Redundant constraint	Presence influence	Practice way of leveling	Leveling absence consequences
1	2	3	4
q_1	Impossibility of self-installation of the pad 3 on the piston 5 [q_1], the pad 2 on the caliper bracket 4 [q_3], and both pads on the disk 2 [q_5] around the X axis [$f_x^{"} = 0$], in the presence of non-parallelism $\Delta\chi$ of the working surfaces of the pads, non-perpendicularity of the piston end to its axis, and the pressure surface of the caliper bracket to the axis of the hydraulic cylinder (Figure 3a).	Deformation of the mechanism parts during their operation.	Uneven pressure distribution at the joints of the mechanism links, their uneven wear, and fluctuations in the friction torque created by the mechanism within the wheel rotation.
q_3			
q_5			
q_2	Impossibility of self-installation of pad 3 on piston 5 [q_2], pad 2 on caliper bracket 4 [q_4], and pads on disk 2 [q_6] around the Y axis [$f_y^{*} = 0$], in the presence of non-parallelism $\Delta\gamma$ of the working surfaces of the pads, non-perpendicularity of the piston end to its axis, and of the caliper bracket surface to the axis of the hydraulic cylinder (Figure 3b).		
q_4			
q_6			
q_9	Impossibility of self-installation of pads 2 [q_9, q_{11}] and 3 [q_{13}, q_{15}] on brake disc 1 around the X axis [$f_x^{"} = 0$], in the presence of end runout of disc 1, uneven wear of the disc ends or working surfaces of the pads, presence of angular errors in the location of the grooves $\Delta\chi$ for the brake pads or pad spikes in the YZ plane (Figure 3c).	Increase in linear gaps gy in kinematic pairs A, B, K, L in the direction of the Y axis.	The presence of mounting stresses in the brake pads of the mechanism, their uneven wear, and fluctuations in the friction torque of the mechanism within the wheel rotation. The occurrence of dynamic loads on the mechanism due to the presence of gaps.
q_{11}			
q_{14}			
q_{15}			
q_7	Impossibility of assembling the $A_3D_3B_3A_3$ [q_7], $A_3C_3B_3A_3$ [q_{10}], $K_3E_3L_3K_3$ [q_{14}] circuits without tension along the Y axis [$f_y^{'} = 0$], in the presence of errors in the location Δy of the grooves for the brake pads or the pad spikes (Figure 3d).		
q_{10}			
q_{12}			
q_8	The impossibility of assembling the pads 2, 3 with the caliper bracket 4 without tension around the Z axis [$f_z^{*} = 0$], in the presence of angular errors $\Delta\xi$ in the location of the grooves for the brake pads or the pad spikes (Figure 3e).		
q_{13}			

https://doi.org/10.14669/AM/218873

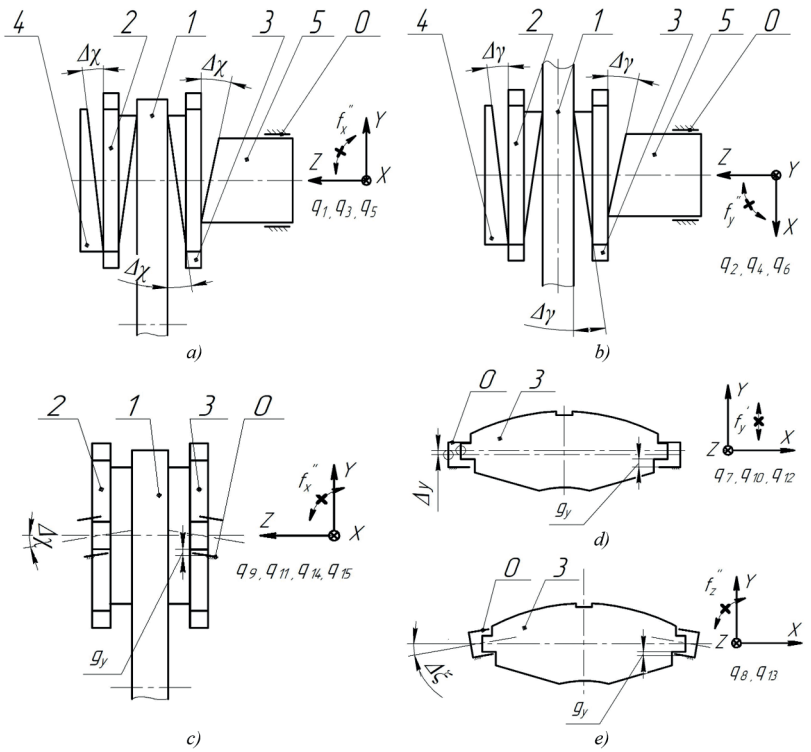

Fig. 3. Schemes for of redundant constraints influence and leveling in basic wheel brake mechanism construction: q1, q3, q5 (a); q2, q4, q6 (b); q9, q11, q14, q15 (c); q7, q10, q12 (d); q8, q13 (e) (markings explanation – in Table 1)

The obtained results support the feasibility of modifying the brake mechanism structure in order to improve its performance, in particular by ensuring the ability of the brake pads to self-align with the discs under varying operating conditions. Among the possible approaches to eliminating redundant constraints, the following should be noted: increasing the class of kinematic pairs (or using kinematic joints), reducing the number of kinematic loops in the mechanism, and decreasing the number of local constraints.

3. Results and discussion

One practical way to reduce the number of redundant constraints is to replace the prismatic guide lugs of the brake pads with cylindrical ones, as well as to introduce spherical supports 6 and 7 into the brake mechanism design. These supports interact with the non-working side surfaces of the brake pads by means of their flat surfaces, and with corresponding bores in the piston and the caliper bracket by means of their spherical surfaces (Figure 4).

https://doi.org/10.14669/AM/218873

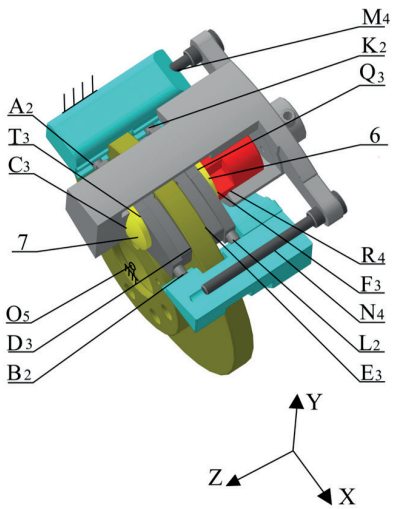

Fig. 4. Modified by the variant 1 wheel brake mechanism structural diagram: 6, 7 – spherical supports

In this (variant 1) construction number of movable links is $n = 7$. 3-class kinematic pairs A_3, B_3, L_3, K_3 became 2-class pairs, and also two spherical 3-class pairs Q_3, T_3 will be added. Therefore the number of 5-class kinematic pairs $P_5 = 1$ [O_5], 4-class kinematic pairs number $P_4 = 3$ [M_4, N_4, R_4], 3-class kinematic pairs number $P_3 = 6$ [C_3, D_3, E_3, F_3, Q_3, T_3], 2-class pairs number $P_2 = 4$ [A_2, B_2, K_2, L_2], 1-class pairs are absent – $P_1 = 0$.

Total kinematic pairs number:

$$P = P_5 + P_4 + P_3 + P_2 + P_1 = 1 + 3 + 6 + 4 + 0 = 14.$$

The sum of kinematic pairs movabilities:

$$f = 1P_5 + 2P_4 + 3P_3 + 4P_2 + 5P_1 = 1\times1 + 2\times3 + 3\times6 + 4\times4 + 5\times0 = 41.$$

Number of independent locked circuits:

$$k = P - n = 14 - 7 = 7.$$

Total mechanism mobility $W = W_b + W_l = 1 + 5 = 6$,

where $W_b = 1$ – basic mechanism mobility (disc 1 rotation);
$W_l = 5$ – local links mobilities (piston 5 and supports 6, 7 rotation; pads 2, 3 moving).

https://doi.org/10.14669/AM/218873

Redundant constraints number in modified by the variant 1 mechanism by Somov and Malyshev formula:

$$q_{SM} = W + 5P_5 + 4P_4 + 3P_3 + 2P_2 + P_1 - 6n = \\ = 6 + 5\times1 + 4\times3 + 3\times6 + 2\times4 + 0 - 6\times7 = 7.$$

Redundant constraints number by Ozols formula:

$$q_{OZ} = W + 6k - f = 6 + 6\times7 - 41 = 7.$$

The circuit method certifies the obtained results (Table 3).

Tab. 3. Circuit method application to the modified by the variant 1wheel brake mechanism basic construction

Circuit	Planar movabilities f_p	Non-planar movabilities f_n
	f_x' f_y' f_z''	f_x'' f_y'' f_z'
$R_4Q_3F_3E_3D_3C_3T_3R_4$	$W_t(6)$ F F QR $W_t(5)$ F	Q Q R
$M_4T_3C_3D_3O_5M_4$	D Ø MT $W_t(7)$ C	T T M
$N_4T_3C_3D_3O_5N_4$	Ø D NO $W_b(1)$ D	Ø Ø N q_1 q_2
$A_2D_3B_2A_2$	$W_t(2)$ AB Ø AB	Ø A A q_3
$A_2C_3B_2A_2$	C C Ø q_4	Ø B B q_5
$K_2F_3L_2K_2$	$W_t(3)$ KL Ø KL	Ø K K q_6
$K_2E_3L_2K_2$	E E E	Ø L L q_7
	$W = 6, q = 7$	

The number of redundant constraints can be further reduced by making the studs of the pads spherical (or barrel-shaped) instead of cylindrical (Figure 5) and increasing the class of the corresponding pairs to the first (the variant 2). In such a construction, the number of movable links will also be $n = 7$. The number of kinematic pairs of the 5-class will be $P_5 = 1$ [O_5], 4-class kinematic pairs number $P_4 = 3$ (M4, N4, R4), 3-class kinematic pairs number $P_3 = 6$ [C_3, D_3, E_3, F_3, Q_3, T_3], 2-class pairs are absent $P_2 = 0$, 1-class kinematic pairs number – $P_1 = 4$ [A_1, B_1, K_1, L_1].

https://doi.org/10.14669/AM/218873

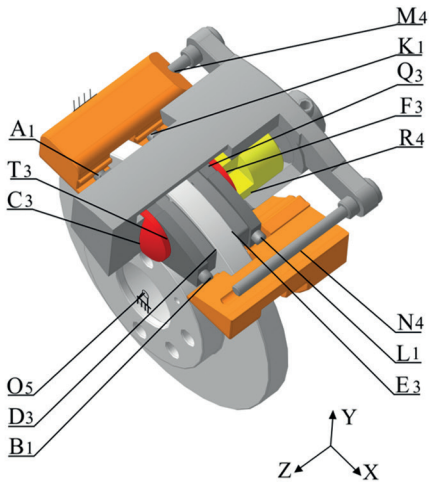

Fig. 5. Modified by the variant 2 brake mechanism structural diagram

Then total kinematic pairs number:

$$P = P_5 + P_4 + P_3 + P_2 + P_1 = 1 + 3 + 6 + 0 + 4 = 14.$$

The sum of kinematic pairs movabilities:

$$f = 1P_5 + 2P_4 + 3P_3 + 4P_2 + 5P_1 = 1\times1 + 2\times3 + 3\times6 + 4\times0 + 5\times4 = 45.$$

Number of independent locked circuits:

$$k = P - n = 14 - 7 = 7.$$

Total mechanism mobility $W = W_b + W_l = 1 + 5 = 6$ (the same as in the variant 1).

Redundant constraints number in number in modified by the variant 2 mechanism by Somov and Malyshev formula:

$$q_{SM} = W + 5P_5 + 4P_4 + 3P_3 + 2P_2 + P_1 - 6n = \\ = 6 + 5\times1 + 4\times3 + 3\times6 + 2\times0 + 4 - 6\times7 = 3.$$

Redundant constraints number by Ozols formula:

$$q_{OZ} = W + 6k - f = 6 + 6\times7 - 45 = 3.$$

To confirm the calculations, Table 4 shows the application of the circuit method.

https://doi.org/10.14669/AM/218873

Tab. 4. The circuit method application to modified by the variant 2 wheel brake mechanism basic construction

Circuit	Planar movabilities f_p	Non-planar movabilities f_n
$R_4Q_3F_3E_3D_3C_3T_3R_4$ $M_4T_3C_3D_3O_5M_4$ $N_4T_3C_3D_3O_5N_4$ $A_1D_3B_1A_1$ $A_1C_3B_1A_1$ $K_1F_3L_1K_1$ $K_1E_3L_1K_1$	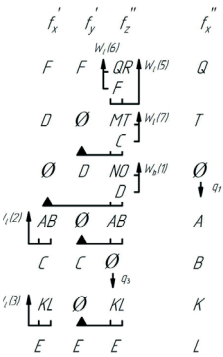	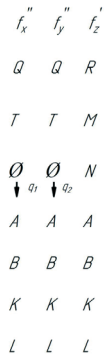

$W = 6, q = 3$

Further modification (the variant 3) is possible by installing the caliper guides 8 and 9 on spherical joints S_3 та V_3 in combination with spherical pad studs and piston thrust on the non-working side surface of the inner brake pad through the spherical support 6 (Figure 6). In this variant of mechanism modification the number of movable links became $n = 8$, 5-class kinematic pairs number will be $P_5 = 1$ [O_5], 4-class kinematic pairs number $P_4 = 3$ [M_4, N_4, R_4], 3-class kinematic pairs number $P_3 = 7$ [C_3, D_3, E_3, F_3, T_3, S_3, V_3], 2-class pairs are absent $P_2 = 0$, 1-class pairs number – $P_1 = 4$ [A_1, B_1, K_1, L_1].

Total kinematic pairs number:

$$P = P_5 + P_4 + P_3 + P_2 + P_1 = 1 + 3 + 7 + 0 + 4 = 15.$$

The sum of kinematic pairs movabilities:

$$f = 1P_5 + 2P_4 + 3P_3 + 4P_2 + 5P_1 = 1\times1 + 2\times3 + 3\times7 + 4\times0 + 5\times4 = 48.$$

Number of independent locked circuits:

$$k = P - n = 15 - 8 = 7.$$

Total mechanism mobility $W = W_b + W_l = 1 + 6 = 7$,

where $W_b = 1$ – basic mechanism mobility (disc 1 rotation);
$W_l = 6$ – local links mobilities (piston 5, support 6 and guides 7, 8 rotation; pads 2, 3 moving).

https://doi.org/10.14669/AM/218873

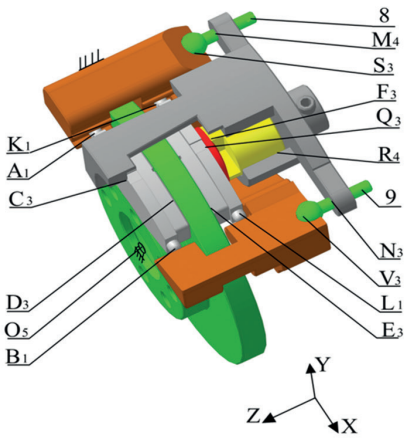

Fig. 6. Modified by the variant 3 brake mechanism structural diagram: 6 – spherical support; 8, 9 – caliper guides

Redundant constraints number in number in modified by the variant 3 mechanism by Somov and Malyshev formula:

$$q_{SM} = W + 5P_5 + 4P_4 + 3P_3 + 2P_2 + P_1 - 6n = \\ = 7 + 5\times1 + 4\times3 + 3\times7 + 2\times0 + 1\times4 - 6\times8 = 1.$$

Redundant constraints number by Ozols formula:

$$q_{OZ} = W + 6k - f = 7 + 6\times7 - 48 = 1.$$

.

The application of the circuit method for the described mechanism is given in Table 5.

Tab. 5. The Circuit method application to modified by the variant 3 wheel brake mechanism basic construction

Circuit	Planar movabilities f_p	Non-planar movabilities f_n
$R_4T_3F_3E_3D_3C_3R_4$	$f_x'\ f_y'\ f_z''$ $W_t(6)$ $F\ F\ FR\ W_t(5)$ T	$f_x''\ f_y''\ f_z'$ $T\ T\ R$
$S_3M_4C_3D_3O_5S_3$ $V_3N_4T_3F_3E_3O_5V_3$	$W_t(7)$ $D\ D\ SO\ W_0(1)$ MD	$S\ S\ M$
$A_1D_3B_1A_1$	$Ø\ Ø\ VN\ W_t(8)$ q_1 $AB\ Ø\ AB$	$V\ V\ N$ $A\ A\ A$
$A_1C_3B_1A_1$	$C\ C\ C$	$B\ B\ B$
$K_1F_3L_1K_1$ $K_1E_3L_1K_1$	$KL\ Ø\ KL$ $E\ E\ E$	$K\ K\ K$ $L\ L\ L$
	$W = 7, q = 1$	

https://doi.org/10.14669/AM/218873

The feasibility of using the described mechanisms in practice can be verified by performing feasibility studies and conducting bench or full-scale experiments. It is also possible to reduce the number of redundant constraints by reducing the number of kinematic pairs, which can be implemented by using a different principle of operation and transmission mechanism between the power hydraulic cylinder and the brake pads.

4. Conclusions

1. The results of a structural analysis of an automotive disc-type wheel brake mechanism are presented. It has been established that this basic mechanism contains $q = 15$ redundant constraints, which may significantly affect its operation.

2. It is shown that the existing redundant constraints may cause off-design loading, in particular assembly and operation with unintended preloads and tensions, and also reduce the uniformity of load distribution among the mechanism components, thereby decreasing the service life of brake parts and potentially reducing the safety of the vehicle braking process;

3. It is shown that, in practice, the influence of redundant constraints is compensated for by increasing clearances in kinematic pairs, which leads to delayed brake actuation and additional dynamic loads during operation, and consequently further reduces durability;

4. A comprehensive improvement in the technical level of disc-type brake mechanisms is achievable through materials science and design approaches, aimed at increasing the wear resistance of friction pairs and the uniformity of load distribution between them; however, the elimination of redundant constraints in the mechanism plays a crucial role in the successful implementation of materials-based solutions;

5. Within the framework of design-based improvements, three variants of new wheel brake mechanism designs are proposed, in which the number of redundant constraints was reduced from $q = 15$ in the basic construction to $q = 7$, $q = 3$, and $q = 1$, which may have a significant positive influence on their functional performance.

5. References

[1] United Nations Economic Commission for Europe (UNECE). Regulation No. 102 – Uniform provisions concerning the approval of vehicles with regard to their straight-line stability: E/ECE/324 Rev. 2/Add. 101. Geneva: UNECE; 2025. Available from: https://unece.org/fileadmin/DAM/trans/main/wp29/wp29regs/r102e.pdf (accessed on 2025 Jan 30).

[2] Li H, Wang K, Hao H, Wu Z. Yaw Moment Control Based on Brake-by-Wire for Vehicle Stability. World Electric Vehicle Journal. 2023;14(9):256. https://doi.org/10.3390/wevj14090256.

[3] Chen J, Liu Y, Liu R, Xiao F, Huang J. Integrated control of braking-yaw-roll stability under steering-braking conditions. Scientific Reports. 2023;13(1):21110. https://doi.org/10.1038/s41598-023-48535-1.

[4] Zhou J, Di Y, Miao X. Single-wheel failure stability control for a vehicle equipped with brake-by-wire system. World Electric Vehicle Journal. 2023;14(7):177. https://doi.org/10.3390/wevj14070177.

[5] Geng H, Hu J, Shen K, Yan F, You Z, Zhang P. Braking force coordination control strategy for electric vehicles considering failure conditions. Applied Sciences. 2025;15(23):12800. https://doi.org/10.3390/app152312800.

[6] Li H, Jin L, Li J, Xiao F, Wang Z, Zhang G. Braking force coordination control for in-wheel motor drive electric vehicles with electro-hydraulic composite braking system. Vehicles. 2025;7(4):119. https://doi.org/10.3390/vehicles7040119.

[7] Jensen KM, Santos IF, Corstens HJP. Prediction of brake pad wear and remaining useful life considering varying vehicle mass and an experimental holistic approach. Wear. 2024;552–553:205433. https://doi.org/ 10.1016/j.wear.2024.205433.

[8] Bevz OV, Magopets SO, Matviienko OO. Study of the characteristics of the braking mechanism of the Hyundai Accent vehicle. Engineering of Agricultural Production, Industry, Machines and Automation. 2019;1(32):68–77. https://doi.org/10.32515/2664-262X.2019.1(32).68-78.

[9] Polajnar M, Kalin M, Thorbjornsson I, Thorgrimsson JT, Valle N, Botor-Probierz A. Friction and wear performance of functionally graded ductile iron for brake pads. Wear. 2017;382–383:85–94. https://doi.org/10.1016/j.wear.2017.04.015.

[10] Ilie F, Cristescu AC. Experimental study of the correlation between the wear and the braking system efficiency of a vehicle. Applied Sciences. 2023;13(14):8139. https://doi.org/10.3390/app13148139.

[11] Kindrachuk M, Volchenko D, Fidrovska N, Dukhota O, Zhuravlev D, Ostashuk M, et al. Wear-friction properties of friction pairs in disc-pad brakes. Eastern-European Journal of Enterprise Technologies. 2023;4(12):56–61. https://doi.org/10.15587/1729-4061.2023.285699.

[12] Ge W, Sun W. Influence of ultrasonic vibration on friction and wear performance of brake disc. Journal of Vibroengineering. 2023;25(3):468–478. https://doi.org/10.21595/jve.2022.22938.

[13] Kazemi H, Du X, Sadjadi H. A method to detect and isolate brake rotor thickness variation and corrosion. International Journal of Prognostics and Health Management. 2023;14(1):3377. https://doi.org/10.36001/ijphm.2023.v14i1.3377.

[14] Zhang S, Hao Q, Liu Y, Jin L, Ma F, Sha Z, et al. Simulation study on friction and wear law of brake pad in high-power disc brake. Mathematical Problems in Engineering. 2019;2019:6250694. https://doi.org/10.1155/2019/6250694.

[15] Boros L, Peter S, Nowak X, Kneissl C, Fischer P. Effects of disc thickness variation and out-of-roundness on electromechanical brakes. Proceedings of Eurobrake 2023. 2023, FISITA, Barcelona, Spain.

[16] Ravliuk VH. Investigation of features of dual wear of pads in brake system of freight cars. Science and Transport Progress. 2019;2(80):111–126. https://doi.org/10.15802/stp2019/166114.

[17] Ravliuk VH, Ravliuk MH, Kyrychenko IK. Statistical processing of brake pads wear parameters of freight cars. Science and Transport Progress. 2020;2(86):74–91. https://doi.org/10.15802/stp2020/203103.

[18] Protsenko V, Malashchenko V, Nastasenko V, Babiy M, Voitovych O. Elevator drum-pad brake mechanisms: redundant constraints and reliability rise opportunity. Scientific Journal of Silesian University of Technology. Series Transport. 2024;125:229–242. https://doi.org/10.20858/sjsutst.2024.125.15.

[19] Bulgakov VM. Theory of mechanisms and machines. Kyiv, TsUL, 2023.

[20] Meneghini L, Noal Artmann V, Simoni R, Simas H. Mobility analysis and self-alignment of a novel asymmetric 3T parallel manipulator. Mechanisms and Machine Science. 2021;94:94–101. https://doi.org/10.1007/978-3-030-60372-4_11.